Szoka, F., & Paphadjopoulos, D. (1978) *Proc. Natl. Acad. Sci. U.S.A. 75*, 4194–4198.
Szoka, F., Jacobson, K., & Papahadjopoulos, D. (1979) *Biochim. Biophys. Acta 551*, 295–303.
Szoka, F., Jacobson, K., Derzko, Z., & Paphadjopoulos, D. (1980) *Biochim. Biophys. Acta 600*, 1–18.
Szoka, F., Magnusson, K.-E., Wojcieszyn, J., Hou, Y., Derzko, Z., & Jacobson, K. (1981) *Proc. Natl. Acad. Sci. U.S.A. 78*, 1685–1689.
Tilcock, C., & Fisher, D. (1979) *Biochim. Biophys. Acta 577*, 53–61.
Wibo, M., & Poole, B. (1974) *J. Cell Biol. 63*, 430–440.
Wilson, T., Papahadjopoulos, D., & Taber, R. (1979) *Cell (Cambridge, Mass.) 17*, 77–84.

Sequence and Structure in Double-Stranded Ribonucleic Acid: $(A\text{-}G\text{-}C\text{-}U)_2$ and $(A\text{-}C\text{-}G\text{-}U)_2$†

Edward Bubienko, Mary Alice Uniack,‡ and Philip N. Borer*

ABSTRACT: Comparative studies of the thermally induced helix–coil transition in ribosyl $(A\text{-}G\text{-}C\text{-}U)_2$ and $(A\text{-}C\text{-}G\text{-}U)_2$ are described. Ordered structures form at low temperatures where the ribofuranose rings adopt the 3′-endo conformation and both oligomer helices have base-paired stacking arrangements qualitatively similar to the A-RNA family configuration. Especially for $(A\text{-}C\text{-}G\text{-}U)_2$, there is a lack of quantitative agreement between the A-family base overlap and the ^1H NMR data; ring-current and atomic diamagnetic anisotropies using A-form structures fail to predict five of the seven aromatic C–H resonances within 0.2 ppm. The NMR results are in better agreement with the A form for $(A\text{-}G\text{-}C\text{-}U)_2$. For both oligomers, the changes in chemical shift for the anomeric (H1′) resonances indicate substantial (≥20°) changes in the average glycosidic torsion angle upon base pairing and stacking for the adenosine and cytidine residues; this angle in uridine and guanosine residues must change only slightly.

Oligonucleotides as models for double-stranded RNA have been studied extensively since the pioneering work of Thach (1966), Martin et al. (1971), and Uhlenbeck et al. (1971), who developed procedures for the preparation of oligomers having a defined sequence. Kearns (1977) and Kallenbach & Berman (1977) have reviewed much of the subsequent literature that developed in the application of physical methods to determining structural and dynamic features of these defined model systems.

NMR[1] is one of the few solution methods that can provide structural information on a detailed atom-by-atom level. Until now much of its potential has gone unrealized because of problems in theoretical interpretation of chemical shift changes when the oligomers undergo a helix–coil transition. It has been difficult to connect these large (up to 1.5 ppm) changes to geometrical features in anything but a qualitative fashion. Nevertheless, it has been shown that these oligo-RNA duplexes conform to the standard ^3E (3′-endo) furanose ring pucker and the general features of the A-RNA family of structures determined by X-ray diffraction in the solid state. Much of the difficulty in the quantitative interpretation of the NMR data stems from an inadequate theoretical description of the local magnetic anisotropy of such functionalities as the phosphate and the furanose ring oxygen as well as effects of solvent exclusion, hydrogen bonding, multiple aggregation, etc. described by Borer et al. (1975).

In several important papers, Giessner-Prettre, Pullman, and co-workers (1976, 1977a,b), Arter & Schmidt (1976), and Kan et al. (1979) accurately considered the spatial dependence of ring current and atomic diamagnetic anisotropies on the aromatic ring and furanose protons. It occurred to us that these new tools in a careful comparative approach could allow us to probe the structural details of oligomer helices as never before. The simple tetranucleotide duplexes $(A\text{-}G\text{-}C\text{-}U)_2$ and $(A\text{-}C\text{-}G\text{-}U)_2$ are easily synthesized in good yield, have simple, easily assigned NMR spectra because of their self-complementary nature, and, in the comparison, might have nearly identical characteristics with respect to the phosphate and furanose anisotropies, solvent exclusion, hydrogen bonding, multiple aggregation, etc. that plague studies that depend on de novo application of NMR principles to a single oligomer.

We find that both duplexes belong to the A-RNA family of structures with a ^3E sugar pucker and the general features of A-form base stacking. However, $(A\text{-}C\text{-}G\text{-}U)_2$ clearly does

† From the Department of Chemistry, University of California at Irvine, Irvine, California 92717. *Received April 29, 1981.* This work was supported in part by a grant from the National Institutes of Health (GM-24494). A grant from the National Science Foundation (CHE 79-10821) provided funds for the Bruker WM-250. Experiments with the 500-MHz instrument were performed at the Southern California Regional NMR Facility at California Institute of Technology established by National Science Foundation Grant CHE 7916324. E.B. was supported by a U.S. Public Health Service predoctoral training grant (GM-07311-5).

‡ Present address: Department of Biochemistry, University of Illinois, Urbana, IL 61801.

[1] Abbreviations and symbols used: NMR, nuclear magnetic resonance; HPLC, high-pressure liquid chromatography; FT, Fourier transform; δ, chemical shift; $J_{1'-2'}$, ribose H1′–H2′ coupling constant; J_{5-6}, base H5–H6 coupling constant; Pu, purine; Py, pyrimidine; A-G-C-U and A-C-G-U, ribosyl ApGpCpU and ApCpGpU, respectively (the standard 3′–5′ phosphodiester linkage is implied in this notation for these and other oligoribonucleotides); CDP, cytidine 5′-diphosphate; GDP, guanosine 5′-diphosphate; UDP, uridine 5′-diphosphate; PNPase, primer-independent polynucleotide phosphorylase (*M. luteus*, EC 2.7.7.8); PNPase P, primer-dependent polynucleotide phosphorylase; RNase A, bovine pancreatic ribonuclease (EC 3.1.27.5); RNase T_1, ribonuclease T_1 (*A. oryzae*, EC 3.1.27.5); BAPase, bacterial alkaline phosphatase (*E. coli*, EC 3.1.3.1); Hepes, *N*-(2-hydroxyethyl)piperazine-*N*′-2-ethanesulfonic acid; Tris-HCl, tris(hydroxymethyl)aminomethane hydrochloride; TEAB, triethylammonium bicarbonate; EDTA, ethylenediaminetetraacetic acid; DSS, 4,4-dimethyl-4-silapentane-1-sulfonate; DEAE-Sephadex, diethylaminoethyl-Sephadex A-25.

0006-2960/81/0420-6987$01.25/0

not conform to the A-form stacking pattern in detail. We do not yet propose an alternate structure but are currently progressing with a detailed model building study which should provide the appropriate overlap. We believe this is the first time conclusive evidence has been presented to show that RNA double helices can exist in nonstandard solution forms. Nonstandard RNA helical forms have been shown to occur in the solid state (Chandrasekaran et al., 1980). We can successfully rationalize the δ vs. temperature changes observed for the H1′ protons upon duplex formation in terms of changes in the glycosidic torsion angle. In $(A\text{-}G\text{-}C\text{-}U)_2$ and $(A\text{-}C\text{-}G\text{-}U)_2$, A and C exhibit large changes in average glycosidic angle upon base pairing and stacking while U and G are apparently less sensitive.

Materials and Methods

Synthesis. The syntheses of A-G-C-U and A-C-G-U follow previously published procedures (Borer, 1972; Borer et al., 1975). Small scale trial reactions in the chain elongation steps were performed to optimize reaction conditions and yields. The constituents of these reactions were analyzed by using HPLC techniques as developed by McFarland & Borer (1979).

A-G-C Preparation. The dimer ApG was purchased as the ammonium salt (Sigma) and used without further purification. A solution (23.3 mL) containing 3.0 mM ApG [ϵ_{260} = 25.0 A_{260} units/μmol of strand at 25 °C (Borer, 1975)], 35 mM CDP, 10 mM $MgCl_2$, 0.4 M NaCl, 0.2 M Hepes (pH 8.2), 10% (v/v) PNPase P, and 1000 units/mL RNase A was incubated for 16 h at 37 °C. This mixture was placed in a boiling water bath for 9 min to denature the PNPase P and subsequently treated for 4 h with bacterial alkaline phosphatase (130 μg/mL, Worthington) to degrade any remaining CDP and yield ApGpC. As a preliminary purification step, the contaminating enzymes were removed on a Bio-Gel P-10 (100–200 mesh) column (3.4 × 46 cm) with 7 M urea, 50 mM NaCl, and 10 mM Tris-HCl (pH 8.2) as the elution medium. A-G-C was purified on a DEAE-Sephadex–HCO_3^- (Pharmacia, A-25) anion-exchange column (1.4 × 46 cm) with a 1.8-L linear gradient from 0.01 to 0.50 M TEAB.

A-G-C-U Preparation. A solution (38.3 mL) containing 1.0 mM A-G-C [ϵ_{260} = 30.9 A_{260} units/μmol of strand at 25 °C (Borer, 1975)], 17.5 mM UDP, 10 mM $MgCl_2$, 0.8 M NaCl, 0.2 M glycine–NaOH (pH 9.3), and 10% (v/v) PNPase P was incubated for 25 min at 37 °C. This mixture was placed in a boiling water bath for 10 min to inactivate the PNPase P and subsequently treated with BAPase to degrade any remaining UDP and yield A-G-C-U_n oligomers. The resulting A-G-C-U_n reaction mixture was separated on a DEAE-Sephadex–Cl^- (Pharmacia, A-25) anion-exchange column (2.3 × 46 cm) with a 2-L linear gradient from 0.0 to 0.5 M NaCl in 7 M urea and 0.01 M Tris-HCl (pH 8.2). The urea was removed on a DEAE-Sephadex–Cl^- column (2.1 × 6.5 cm) by first binding the oligomers and rinsing with 0.1 M NaCl and 0.01 M Tris-HCl (pH 8.2) and followed by 0.4 M NaCl and 0.01 M Tris-HCl (pH 8.2) to elute the oligomers. The different oligomer fractions were desalted on a Bio-Gel P-2 (50–100 mesh) column (5.5 × 60 cm) with "Milli-Q" (Millipore Corp.) deionized water at a flow rate of 10 mL/min. The samples were evaporated under vacuum and quantitated by absorbance at 260 nm. A total of 8 μmol of A-G-C-U [ϵ_{260} = 39.9 A_{260} units/μmol of strand at 25 °C (Borer, 1975)] was isolated.

A-C-G Preparation. The dimer ApC was purchased as the ammonium salt (Sigma) and used without further purification. A solution (18.8 mL) containing 3.0 mM ApC [ϵ_{260} = 21.0 A_{260} units/μmol of strand at 25 °C (Borer, 1975)], 35 mM GDP, 10 mM $MgCl_2$, 0.4 M NaCl, 0.2 M Tris-HCl (pH 8.2), 10% (v/v) PNPase P, and 1000 units/mL RNase T_1 was incubated for 48 h at 37 °C. PNPase P was heat denatured as before, and then BAPase was added as before followed by heat denaturation. A-C-G was separated from the other reaction components on a DEAE-Sephadex–HCO_3^- (Pharmacia, A-25) anion-exchange column (1.4 × 46 cm) with a 2-L linear gradient from 0.01 to 0.60 M TEAB.

A-C-G-U Preparation. A solution (8.3 mL) containing 1.0 mM A-C-G [ϵ_{260} = 31.6 A_{260} units/μmol of strand at 25 °C (Borer, 1975)], 17.5 mM UDP, 10 mM $MgCl_2$, 0.8 M NaCl, 0.2 M Hepes (pH 8.2), and 10% (v/v) PNPase P was incubated for 60 min at 37 °C. This mixture was placed in a boiling water bath for 10 min to denature the PNPase P and subsequently treated with BAPase to degrade any remaining UDP and yield A-C-G-U_n oligomers. Again, the reaction solution was placed in a boiling water bath to inactivate the BAPase. The resulting mixture of A-C-G-U_n oligomers was separated on a DEAE-Sephadex–Cl^- (Pharmacia, A-25) anion-exchange column (2.3 × 46 cm) with a 2-L linear gradient from 0.0 to 0.5 M NaCl in 0.01 M Tris-HCl (pH 8.2). A-C-G-U was desalted by elution on a Bio-Gel P-2 (50–100 mesh) column (2.3 × 46 cm) as before and evaporated under vacuum and quantitated by absorbance at 260 nm. A total of 1.6 μmol of A-C-G-U [ϵ_{260} = 41.3 A_{260} units/μmol of strand at 25 °C (Borer, 1975)] was isolated.

Proof of Sequence. The sequence integrity of the oligomeric products and intermediates was carefully checked after each synthetic step. RNase A, RNase T_1, and BAPase were used in combinations in a series of verification reactions. The verification products along with authentic markers were analyzed and quantitated by using HPLC techniques (McFarland & Borer, 1979) giving the predicted products and ratios. Additional support for the identity of the oligomeric products and some of their intermediates was generated by an analysis of their ^{1}H NMR spectra.

Proton Magnetic Resonance. The NMR samples were 3 mM in strand concentration, 0.10 M NaCl, 0.01 M phosphate buffer (pH 7.2), and 10^{-4} M EDTA (Borer et al., 1975). The exchangeable protons were replaced with deuterium by dissolving the samples in 2 mL of distilled D_2O of 99.7 or 99.8 atom % of D minimum isotopic purity (Merck or Aldrich) and evaporating the resulting solution to dryness under vacuum (repeated 4 times). The final samples were prepared by dissolving them in 99.96 atom % D minimum isotopic purity D_2O (Aldrich) and adding 5 μL of 4.5 M *tert*-butyl alcohol in 99.96% D_2O as an internal reference. Sample volumes were 0.3–0.5 mL. Chemical shifts were reported with respect to DSS as described in Borer et al. (1975).

The proton magnetic resonance spectra were recorded on various spectrometers operating in the quadrature FT mode. The instruments used were the following: a Varian HR-220, a Bruker WM-250, a Nicolet NT-360, and a Bruker WM-500. The instrumental parameters that were used have been previously cited (Stone et al., 1981). Temperatures (±1 °C) were verified by reference to methanol or ethylene glycol standards (Van Geet, 1968, 1970).

Results

General Characteristics of the Base and Ribose H1′ NMR Spectra. An illustration of a 220-MHz ^{1}H NMR spectrum of A-G-C-U at 41 °C (3 mM strand concentration) and a 360-MHz ^{1}H NMR spectrum of A-C-G-U at 40 °C (3 mM strand concentration) is given in Figure 1. At low field (8.4–7.6 ppm), there is a group of five resonances corresponding to the purine H8 and adenine H2 singlets and the

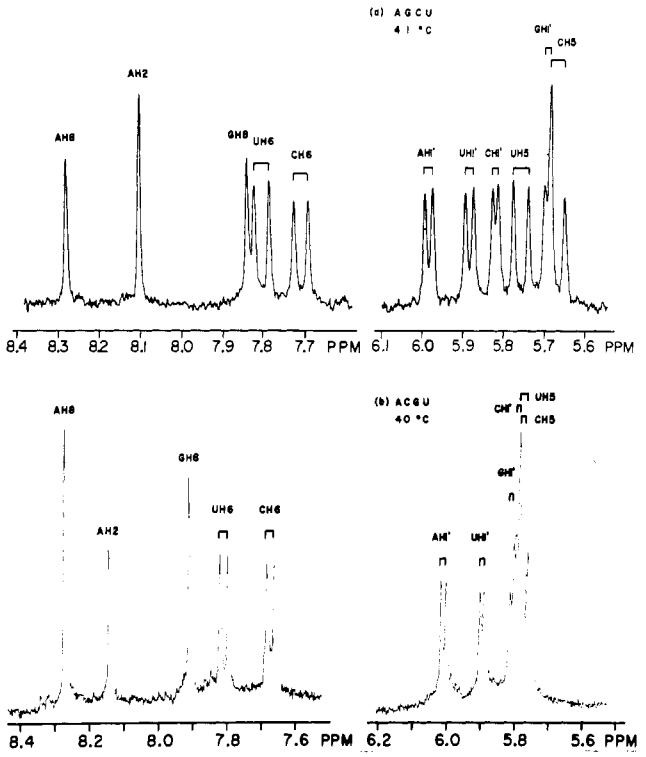

FIGURE 1: ^{1}H NMR spectra of the nonexchangeable base and ribose H1′ protons of (a) A-G-C-U at 220 MHz (41 °C) and (b) A-C-G-U at 360 MHz (40 °C). The samples were 3 mM in strands, 0.11 M Na^+, 0.01 M sodium phosphate buffer (pD 7.2), and 10^{-4} M EDTA in D_2O. Chemical shifts are expressed in reference to DSS.

Table I: Chemical Shift Differences between the Coil and Duplex Forms of A-G-C-U and A-C-G-U[a]

proton	$\delta_{coil} - \delta_{duplex}$[b] A-G-C-U	A-C-G-U	Δ[c]	Δ(m)[d]
AH8	0.00	-0.06	0.06	-0.02
AH2	1.12	0.62	0.50	0.03
GH8	0.57	0.38	0.19	-0.09
CH5	0.73	0.72	0.01	-0.03
CH6	0.13	0.05	0.08	-0.12
UH5	0.25	0.56	-0.31	-0.01
UH6	-0.03	0.15	-0.18	-0.11
AH1′	0.33	0.31	0.02	-0.02
GH1′	0.06	0.05	0.01	-0.05
CH1′	0.43	0.35	0.08	0.02
UH1′	0.14	0.18	-0.04	0.02

[a] In parts per million. The values used in these calculations are found in Table II. [b] A positive value signifies a shielding increase while a negative value signifies deshielding of the duplex form relative to the coil form at 60 °C. [c] These values are the difference between columns 2 and 3. [d] These are the differences between the δ values for mononucleotides at 60 and 0–5 °C (see Table II, notes *b* and *f*).

pyrimidine H6 doublets. At higher field (6.1–5.6 ppm), there is a group of six resonances corresponding to the pyrimidine H5 and ribose H1′ doublets. The general appearance of the A-C-G-U spectra is similar except for important 0.05–0.5-ppm differences in chemical shifts of corresponding protons.

At the higher temperatures, the resonance lines are narrow while as the temperature is lowered the lines broaden (some lines broaden faster than others); hence, the resonances are better dispersed at intermediate and high temperatures [i.e., 30–75 °C for $(A\text{-}G\text{-}C\text{-}U)_2$ and 20–70 °C for $(A\text{-}C\text{-}G\text{-}U)_2$]. The changes in chemical shifts are predominantly upfield as the temperature is lowered. Also, the H1′–H2′ coupling constants ($J_{1'-2'}$) decrease upon lowering the temperature.

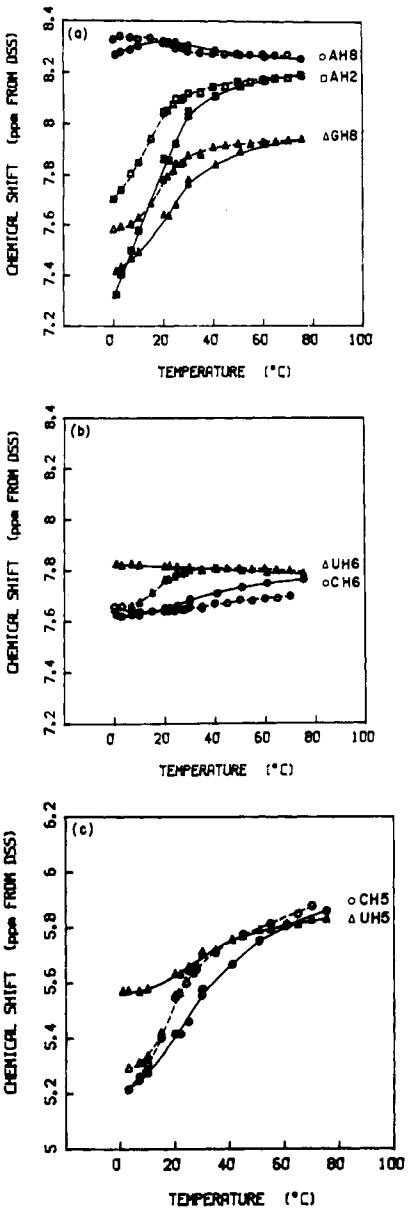

FIGURE 2: Chemical shift vs. temperature for the nonexchangeable base protons of A-G-C-U and A-C-G-U (same sample conditions as in Figure 1): (a) AH8, AH2, and GH8, (b) CH6 and UH6, and (c) CH5 and UH5. The solid symbols represent A-G-C-U and the open symbols represent A-C-G-U.

Effects of Temperature Variation on the Chemical Shifts of the Base and Ribose H1′ Protons. The temperature dependence of these resonances for A-G-C-U and A-C-G-U is summarized in Figures 2 and 3. The figures show the general trend of increased shielding with decreasing temperature just noted. In addition the sigmoid character of most of these plots is diagnostic of a cooperative order–disorder transition with increasing temperature. A further trend that bears upon the effect of sequence on the details of the transition can be noted in the similarity in shape of most of the δ vs. T profiles for corresponding protons. It is interesting that a relative shift of 9–14 °C toward higher temperature nearly superimposes the A-C-G-U profiles on the corresponding A-G-C-U profiles in Figure 2. By contrast, the corresponding H1′ profiles (Figure 3) coincide nicely without any adjustment in temperature.

Table I compares the shielding changes accompanying the order–disorder transition for corresponding protons. The differences in shielding between the duplex and coil forms for the corresponding ribose H1′ are almost identical. The base

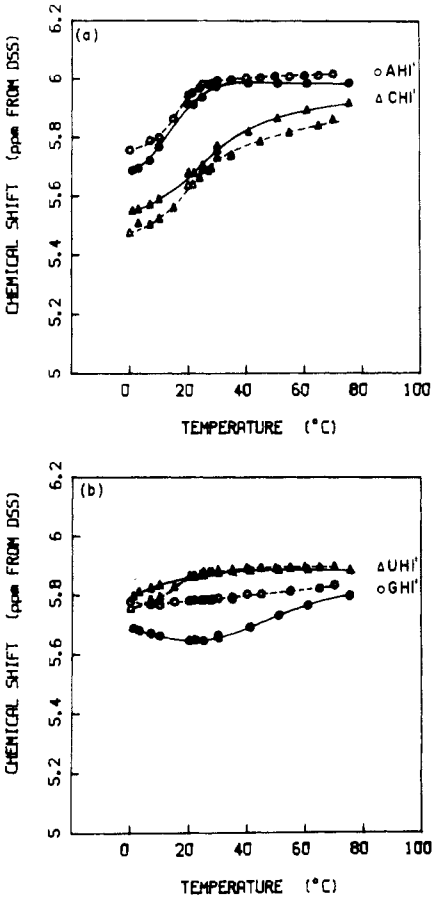

FIGURE 3: Chemical shift vs. temperature for the ribose H1′ protons of A-G-C-U and A-C-G-U (same sample conditions as in Figure 1): (a) AH1′ and CH1′ and (b) GH1′ and UH1′. The solid symbols represent A-G-C-U and the open symbols represent A-C-G-U.

protons show more variation. The greatest differences are for the AH2, UH5, GH8, and UH6.

Temperature Dependence of the Ribose H1′–H2′ Coupling Constants. The ribose H1′–H2′ coupling constants ($J_{1'-2'}$) change with temperature as shown in Figure 4. The $J_{1'-2'}$ values for the AH1′, GH1′, and CH1′ resonances of A-G-C-U and A-C-G-U decrease from approximately 5 Hz to less than 1.5 Hz upon lowering the temperature while the $J_{1'-2'}$ values for the UH1′ resonances at first increase from approximately 3.5 Hz at 80 °C to roughly 4.5 Hz at 50 °C and then decrease to less than 1.5 Hz with decreasing temperature for both molecules. At lower temperatures, the ribose H1′–H2′ coupling constants are less than 1.5 Hz (i.e., the resonances appear as singlets).

Within experimental uncertainty, the $J_{1'-2'}$ vs. temperature profiles for the AH1′, GH1′, and CH1′ protons of A-C-G-U can be superimposed upon the profiles of the corresponding protons of A-G-C-U by shifting the A-C-G-U temperature scale a positive 12–20 °C (see Figure 4). However, the $J_{1'-2'}$ vs. T profiles for UH1′ are directly superimposable without any relative temperature shift (see Figure 4d).

Variation of Line Width with Temperature. With decreasing temperature, particularly in the range of the coil → duplex transition, all of the resonance lines broaden. In addition, some of the signals show a loss in integrated area in comparison to others. The line widths and relative intensities of signals are similar for corresponding protons in A-G-C-U and A-C-G-U. The values we quote below are for a 360-MHz spectrum of A-G-C-U at 3 °C with a repetition rate of 1.6 s. The sharpest lines are the H1′ (about 6 Hz, collapsed doublets) and then for the singlet resonances, AH8 (7 Hz),

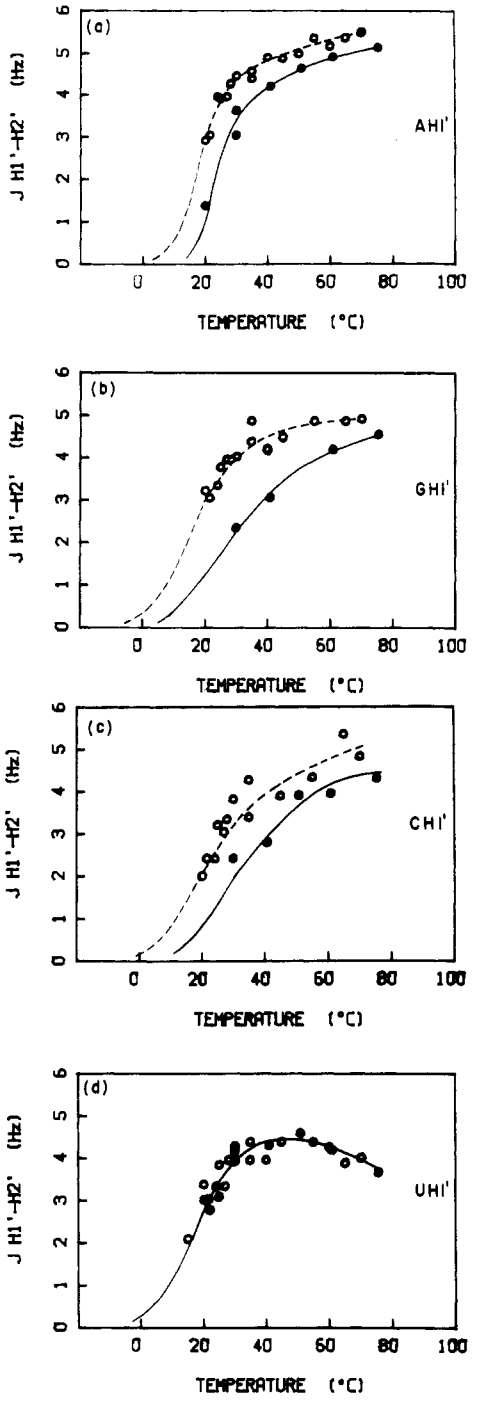

FIGURE 4: $J_{1'-2'}$ vs. temperature for A-G-C-U and A-C-G-U (same sample conditions as in Figure 1): (a) AH1′, (b) GH1′, (c) CH1′, and (d) UH1′. The lowest temperature points indicate the temperature below which the resonances (doublets) become singlets with $J_{1'-2'} \leq$ 1.5 Hz. The solid symbols represent A-G-C-U and the open symbols represent A-C-G-U. It should be noted that the curves are extrapolations at 15 °C and below; $J_{1'-2'}$ is theoretically zero for pure ^{3}E pucker (Dhingra & Sarma, 1979).

GH8 (11 Hz), and AH2 (20 Hz). The pyrimidine doublets are also collapsed with widths at half-height, H6 (10 Hz) and H5 (20 Hz), though the H6 are close to appearing split. The ratios of integrated intensities are about 2/1.5/1.5/1.0/1.0 for H6/H5/H1′/H8/H2 (the number for the broad H2 signal is difficult to determine because of overlap with another peak).

Discussion

Stacking Geometry of the (A-G-C-U)$_2$ and (A-C-G-U)$_2$ Duplexes. Table II collects data on the chemical shifts of the

Table II: Duplex δ and Δδ Values Compared with Calculations for A′-RNA and B-DNA Geometries Using Ring Current and Atomic Diamagnetic Anisotropies; Also δ and Δδ Values for Coil Forms at 60 °C[h]

		duplex		A'_{rc}		A'_{ada}		B_{rc}		coil (60 °C)	
		δ_{obsd}[a]	$\Delta\delta_{obsd}$[b]	$\Delta\delta_{calcd}$[c]	diff[d]	$\Delta\delta_{calcd}$[e]	diff	$\Delta\delta_{calcd}$[f]	diff[d]	δ_{obsd}	$\Delta\delta_{obsd}$[g]
AH8	A-G-C-U	8.265	0.12	-0.03	0.15	0	0.1	0.02	0.10	8.262	0.097
	A-C-G-U	8.33	0.05	-0.03	0.08	0	0.05	0.01	0.04	8.271	0.088
AH2	A-G-C-U	7.05	1.20	0.65	0.55	0.9	0.3	0.51	0.69	8.168	0.114
	A-C-G-U	7.55	0.70	0.27	0.43	0.5	0.2	0.20	0.50	8.172	0.110
GH8	A-G-C-U	7.35	0.78	0.68	0.10	0.9	-0.1	0.15	0.63	7.921	0.120
	A-C-G-U	7.55	0.58	0.23	0.35	0.4	0.2	0.04	0.54	7.931	0.110
CH5	A-G-C-U	5.10	1.01	1.16	-0.15	1.0	0.05	0.55	0.50	5.808	0.276
	A-C-G-U	5.12	0.99	1.43	-0.44	1.5	-0.5	0.63	0.36	5.836	0.248
CH6	A-G-C-U	7.62	0.42	0.35	0.07	0.45	0	0.05	0.37	7.750	0.171
	A-C-G-U	7.64	0.40	0.45	-0.05	0.7	-0.3	0.06	0.34	7.691	0.230
UH5	A-G-C-U	5.56	0.38	0.46	-0.08	0.55	-0.15	0.18	0.44	5.812	0.118
	A-C-G-U	5.25	0.69	1.00	-0.31	1.0	-0.3	0.20	0.25	5.808	0.122
UH6	A-G-C-U	7.825	0.19	0.10	0.09	0.3	-0.1	-0.03	0.22	7.797	0.108
	A-C-G-U	7.66	0.36	0.31	0.05	0.45	-0.1	0.03	0.33	7.808	0.097
AH1′	A-G-C-U	5.66	0.47	0.02	0.45			0.19	0.28	5.985	0.124
	A-C-G-U	5.70	0.43	0.00	0.43			0.11	0.32	6.014	0.095
GH1′	A-G-C-U	5.71	0.23	-0.03	0.26			0.08	0.15	5.765	0.125
	A-C-G-U	5.77	0.17	0.01	0.16			0.01	0.16	5.818	0.072
CH1′	A-G-C-U	5.46	0.52	-0.04	0.56			-0.02	0.54	5.892	0.068
	A-C-G-U	5.48	0.50	-0.04	0.54			0.14	0.36	5.834	0.126
UH1′	A-G-C-U	5.75	0.23	-0.04	-0.02			0.27	0.28	5.887	0.114
	A-C-G-U	5.72	0.26	-0.06	-0.05			0.29	0.31	5.896	0.105

[a] These are the low temperature plateau values of δ at 3 mM strand concentration, pD 7.2, 0.11 M Na^+. [b] $\Delta\delta_{obsd} = \delta_{mononucleotide} - \delta_{obsd}$ is the chemical shift of formation for a proton in the duplex. Appropriate mononucleotide values were selected from the following list (δ in ppm from DSS): ApH2, -H8, and -H1′, 8.252, 8.381, and 6.132, respectively; pGH8 and -H1′, 8.126 and 5.936; pCH5, -H6, and -H1′, 6.110, 8.038, and 5.979; pUH5, -H6, and -H1′, 5.935, 8.015, and 5.982; they were measured in 0.01 M sodium cacodylate buffer, pD 5.9 ± 0.1 in D_2O, and 1 mM in the appropriate 5′-mononucleotide (a 2.0 mM sample of 3′-AMP was also measured). Temperatures were 0–5 °C (Borer et al., 1975). [c] Based on the A′-RNA data given in Arter & Schmidt (1976). An A-RNA model has been described which is very similar in stacking to the A′ model. Its predictions agree within ~0.05 ppm of those shown here for the A′ model. [d] Difference between observed value and calculated value. [e] Based on A′-RNA base overlaps and the 3.4 A isoshielding maps given by Giessner-Prettre & Pullman (1976) which include ring current and local atomic diamagnetic anisotropies. The numbers are rounded to the nearest 0.05 ppm, include only nearest neighbor effects, and do not correct for small deviations from the 3.4 A spacing. [f] Based on the B-DNA data given in Arter & Schmidt (1976). [g] The chemical shift of formation for a proton in the 60 °C coil form. These mononucleotide values were used (see footnote *b* for buffer and nucleotide concentrations): ApH2, -H8, and -H1′, 8.282, 8.359, and 6.109; pGH8 and -H1′, 8.041 and 5.890; pCH5, -H6, and -H1′, 6.084, 7.921, and 5.960; pUH5, -H6, and -H1′, 5.930, 7.905, and 6.001. [h] δ in parts per million from DSS.

nonexchangeable protons in the two oligomers. Included are "chemical shifts of formation", sometimes called "polymerization shifts", which compare the δ value of a proton in an unassociated mononucleotide with its value in the oligomer measured under similar solution conditions. Abbreviated with the symbols Δδ, these shifts indicate relative shielding changes upon duplex (or coil) formation. Positive values of Δδ indicate shielding increases over the reference mononucleotides.

The base overlap pattern largely determines the observed Δδ values for the base protons. The A′-RNA geometry overlaps (Arnott et al., 1973) were used to calculate Δδ values in Table II given in the A'_{ada} columns. Here both ring current and local atomic diamagnetic anisotropies were used in the calculation (Giessner-Prettre & Pullman, 1976). Two other headings in Table II, A'_{rc} and B_{rc}, account for ring-current effects by using the A′-RNA and B-DNA geometries (Arter & Schmidt, 1976). Entries are underlined which differ by more than 0.15 ppm between calculation and experiment.

The A'_{ada} approximation is notably superior to the others. The B-stacking form can be ruled out as only 2 of the 14 base protons are fit within the 0.15-ppm criterion. For $(A\text{-}G\text{-}C\text{-}U)_2$ only AH2 does not fit A'_{ada}, although it is substantially better fit than with A'_{rc}. Except for the H1′ (not included in the ada calculations) where the shielding has always been underestimated by ring current models, the $(A\text{-}G\text{-}C\text{-}U)_2$ data is explained quite well by the A'_{ada} paradigm.

However, the A'_{ada} model describes $(A\text{-}C\text{-}G\text{-}U)_2$ only poorly, predicting five of the seven base protons incorrectly by more than 0.2 ppm. The clear implication is that $(A\text{-}C\text{-}G\text{-}U)_2$ possesses a nonstandard helix form. Work currently in progress in our laboratory will establish the likely form of this helix in solution. To our knowledge, this is the first *clear evidence that RNA duplexes can exist in nonstandard solution conformations.*

Furanose Ring Pucker. Figure 4 illustrates the tendency of all the $J_{1'-2'}$ values to decrease to <1.5 Hz at low temperature. This is presumed to mean that the fraction of 3′-endo (^3E) sugar pucker increases as the ordered structure forms. Using the relation that $\%\ ^3E \simeq 10(10 - J_{1'-2'})$ (Dhingra & Sarma, 1979), we can estimate that $\%\ ^3E \geq 70$–80% for each of the furanose rings at 20 °C; this fraction almost certainly increases at lower temperatures. These large $\%\ ^3E$ values are consistent with stacked RNA structures and further disprove the existence of B-form structures which have ~0% ^3E.

H1′ Chemical Shifts and Glycosidic Torsion Angles. An advantage of a study such as this one where two similar oligomers are compared is that the behavior of corresponding protons can be contrasted. The similarities are striking and the differences often subtle and intriguing. For example, Table I shows that for the corresponding H1′ the overall "height" of the δ vs. *T* profiles was nearly the same. Thus, the change

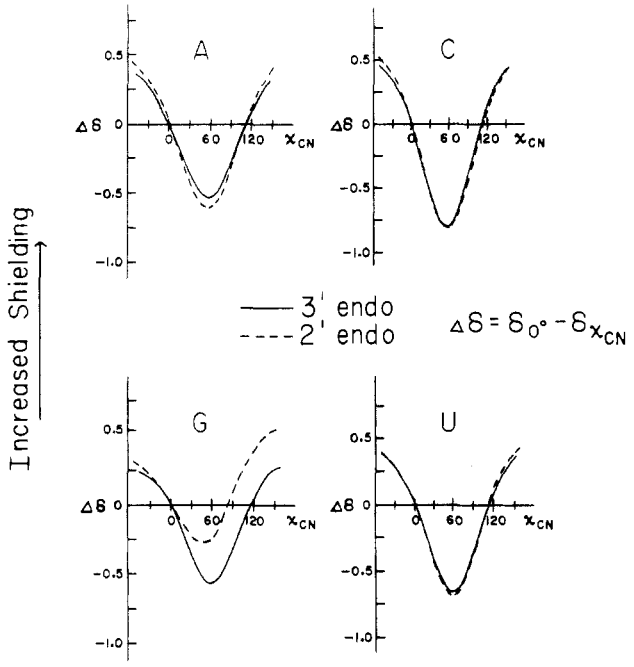

FIGURE 5: Changes in shielding upon variation in glycosidic torsion angle, χ_{CN}. $\Delta\delta$ is defined as zero at $\chi_{CN} = 0°$. Adapted from Giessner-Prettre & Pullman (1977a,b).

in magnetic anisotropy surrounding the H1′ has very little to do with the base sequence or stacking arrangement. No wonder ring-current calculations fit $\Delta\delta$ values for the H1′ so poorly! Table I and Figure 3 clearly show that it is the identity of the base that determines the transition height.

Giessner-Prettre & Pullman (1977a,b) considered the effects of ring current, atomic diamagnetic anisotropy (ada), and polarization (electric field) due to the net charges on neighboring atoms to the ribose protons. Figure 5 shows the effect of variation in the glycosidic torsion angle, χ_{CN}, upon the chemical shift of the H1′. These figures predict decreased shielding as χ increases from 0° through about 60°, and then $\Delta\delta$ increases at angles past 60°. The ada and polarization effects on H1′ arise mainly from the C2 carbonyl (Py) or N3 (Pu) and are much larger than the ring-current effect. Holbrook et al. (1978) analyzed X-ray diffraction data on crystals of yeast $tRNA^{phe}$ and reported χ values for all 72 residues. Averaging χ for residues in helical regions, not near the ends, and involving only the four common nucleotides, it is found that $\chi = 0$–10° with a standard deviation of about 10°. We assume that $(A\text{-}G\text{-}C\text{-}U)_2$ and $(A\text{-}C\text{-}G\text{-}U)_2$ form similar helices to the helical portions of tRNA so the low temperature form should have χ near 0–10° for each residue. Changes in average χ of ~30°, 20°, 10°, and 15° respectively for A, C, G, and U can be inferred from a comparison of Figure 5 and the δ_{coil}–δ_{duplex} data for the H1′ in Table I. This analysis also assumes that an average value of χ can be used for the residues in the coil form. Clearly a wide range of χ values characterize the range of microstates represented in the coil "state", and there is a nonlinear dependence of $\Delta\delta$ on χ. Realizing this we can say that (1) upon melting average χ increases from the 0 to 10° range typical of the helix, (2) the change in average χ is larger for A and C than that for G and U, and (3) it is the *identity* of the base, *not* the *sequence*, that determines the change in χ and consequently $\Delta\delta$ in these tetranucleotide helices.

Line Widths and Integrated Intensities. Previous work on short RNA duplexes has been carried out at higher strand and salt concentrations than the present study. For example, when Borer et al. (1975) studied $(A_2\text{-}G\text{-}C\text{-}U_2)_2$ formation in 1 M NaCl, and 10 mM strands, they noted turbidity in the sample, broadening of lines, and loss of signal intensity at low temperatures. Romaniuk et al. (1978) in a study of G-A-G-C: G-C-U-C at 13 mM strands in 1 M NaCl noted similar effects with precipitation, loss of signal intensity, and severe broadening of all but the AH2 singlet. Speculation in each case suggested that multimolecular aggregates formed and that, in particular, these might be end-to-end aggregates where the purines of two duplexes could stack upon each other. This seemed plausible, especially in view of the anomalously high shielding of the AH2 at the 5′ terminus of $(A_2\text{-}G\text{-}C\text{-}U_2)_2$ that could not be explained by intramolecular ring-current effects. However, this justification is less valid currently as Giessner-Prettre & Pullman (1976) have shown that ada contributions provide additional shielding; the $\Delta\delta_{obsd}$ = 1.36 ppm (Borer et al., 1975) could arise from the neighboring adenine which is now estimated to provide as much as 1.62-ppm shielding.

In the present study, we have reduced strand concentration to 3 mM and [NaCl] to 0.1 M, yet still see severe line broadening and some loss of signal intensity. Turbidity was never observed in these samples. Though this does not prove the absence of the effect, it is not necessary to invoke aggregation as an explanation for line broadening. Perhaps we are observing broadening due to the intrinsic rates of the helix–coil or helix-tightening equilibria.

Furthermore, we can use the data collected by Ts'o (1974) on the dimerization of adenosine to estimate the importance of duplex–duplex stacking upon terminal adenosine residues. If we estimate an equilibrium constant for dimerization of 12.2 M^{-1} at 0 °C from the $K_{25°C}$ and $\Delta H°$ values quoted by Ts'o (1974), the mole fraction of dimers is 0.06 at 3 mM strands and 0.17 at 10 mM. Adenosine monomer can stack another adenosine on either side of the ring plane, so these fractions may overestimate the fraction of end-to-end aggregates in a sample 3 mM in oligonucleotide. The other nucleosides associate less strongly than A; for instance only 0.8% of cytosine should exist as dimers at 0 °C. Thus, oligomers terminating in G-C pairs should have even less tendency to form end-to-end aggregates.

In support of the end-to-end association model, we note that the AH2 line broadens severely in our A-terminal oligomers while it was sharp in $(C\text{-}A\text{-}U\text{-}G)_2$ and G-A-G-C:G-C-U-C (Romaniuk et al., 1978; Hughes et al., 1978) where the A residue was not at the duplex end. It could as easily reflect some difference in the stacking geometry or the dynamic behavior of the duplex, however. Some sort of aggregation certainly can occur because of the turbidity noted at ~10 mM strands; we no longer feel the evidence is strong for end-to-end association between duplexes.

Our data on line widths and relative intensities suggest that the motions of the AH8 and the H1′ are restricted to areas of space not near other protons. AH2 and the PyH5, on the other hand, are efficiently relaxed, implying proximity to other protons. The PyH6 and GH8 exhibit intermediate relaxation properties. These duplexes are simple enough in their spectra that it should be possible to accurately measure relaxation times and nuclear Overhauser enhancements to learn more about their structures and dynamics.

Conclusions about $(A\text{-}G\text{-}C\text{-}U)_2$ and $(A\text{-}C\text{-}G\text{-}U)_2$ Conformation. (1) The A′-RNA (or A-RNA) base-stacking geometry fits $(A\text{-}G\text{-}C\text{-}U)_2$ quite well but $(A\text{-}C\text{-}G\text{-}U)_2$ only qualitatively; $(A\text{-}C\text{-}G\text{-}U)_2$ clearly possesses a nonstandard form. Incorporation of atomic diamagnetic anisotropies improves the quality of fit obtained by ring-current calculations. (2) Both

Table III: Chemical Shifts (in ppm) of the Nonexchangeable Base and Ribose H1′ Protons for ApG, ApGpC, ApGpCpU, CpU, ApCp, ApCpGpU, and GpU at 67 °C along with the Appropriate Coupling Constants (in Hz)[a]

	sequence						
proton	ApG	ApGpC	ApGpCpU	CpU	ApCp	ApCpGpU	GpU
AH8	8.243	8.251	8.260		8.270	8.268	
AH2	8.193	8.179	8.180		8.176	8.177	
GH8	7.944	7.932	7.936			7.933	7.974
CH5		5.856 (7.6)	5.839 (7.6)	6.004 (7.5)	5.839 (7.6)	5.861 (7.5)	
CH6		7.767 (7.6)	7.758 (7.6)	7.815 (7.8)	7.712 (7.6)	7.697 (7.5)	
UH5			5.824 (8.0)	5.861 (8.2)		5.815 (8.0)	5.809 (7.9)
UH6			7.794 (8.0)	7.848 (8.2)		7.806 (8.0)	7.804 (7.9)
AH1′	5.972 (4.6)	5.980 (4.9)	5.985 (5.0)		6.001 (5.2)	6.013 (5.5)	
GH1′	5.841 (4.6)	5.801 (4.3)	5.782 (4.3)			5.825 (4.9)	5.894 (4.9)
CH1′		5.885 (4.9)	5.909 (4.3)	5.852 (3.8)	5.868 (4.9)	5.851 (4.8)	
UH1′			5.886 (4.1)	5.903 (3.2)		5.894 (4.1)	5.899 (3.4)

[a] Coupling Constants shown in parentheses are J_{5-6} for C and U and $J_{1'-2'}$ for A, G, C, and U.

oligomers form duplexes with the ^{3}E sugar pucker, consistent with the A-family structure. (3) The variation of δ for the H1′ can be interpreted by increases in average glycosidic torsion angles of $\geq 20°$ for A and C upon helix melting. G and U change their χ angle very little upon disruption of base pairing and stacking. (4) In the low temperature duplex forms, the motions about AH2 and the PyH5 are constrained near other protons whereas the H1′ and AH8 are in regions of space not near other protons. (5) There are interesting similarities and differences in the proton-by-proton comparison of the two oligomers that appear in the δ and $J_{1'-2'}$ vs. temperature profiles. These bear on conformation and the details of helix melting and are the subject of additional papers in this series (E. Bubienko and P. N. Borer, unpublished results).

Assignments. The chemical shift data that were used in the assignment procedure are found in Table III. There are several general guidelines which are used in the assignment of the resonance signals (Borer et al., 1975).

A-G-C-U. The "incremental assignment" method as described by Borer et al. (1975) was used for correlating particular base or ribose H1′ protons with their resonances. The resonances of corresponding protons usually agree within 0.05 ppm if they are distant from the newly added residue. Occasional reference to coupling constant data or temperature dependence is necessary to establish assignments where two or more are within 0.05 ppm of each other. The complete and unambiguous assignment of the ApG resonances was made by Lee et al. (1976). The assignments for ApG in the present study are in agreement with those of Lee et al. (1976) and Everett et al. (1980). Also, for A-G, the AH2 resonance was unambiguously assigned since AH8 and GH8 are relatively more acidic than AH2; the former exchange with D_2O faster at high temperatures, resulting in lower signal intensities for AH8 and GH8 relative to AH2 after a heating cycle. The assignments for A-G-C are in agreement with those of Everett et al. (1980). The CH5 of A-G-C was unambiguously assigned by using homonuclear decoupling from the CH6. In A-G-C-U the CH6 and UH6 protons were unambiguously assigned using J_{5-6} data. Again, the CH5 and UH5 protons of A-G-C-U were unambiguously assigned by using homonuclear decoupling data.

For the H1′ signals, GH1′ in A-G-C is assigned to the most shielded resonance at 5.80 ppm. It is slightly upfield from 5.84 ppm in A-G, perhaps more shielded as a result of adding the new neighbor C. The other two resonances are substantially less shielded at 5.98 and 5.89 ppm. The former is assigned to AH1′ and is similar to the 5.97 ppm observed in A-G, leaving the 5.89-ppm resonance as CH1′. In A-G-C-U it is easy to assign AH1′ and GH1′ to corresponding A-G-C signals. However, there is some ambiguity in distinguishing CH1′ and UH1′ which are assigned at 5.91 and 5.89 ppm, respectively. The 5.89-ppm resonance is the position of CH1′ in A-G-C. To resolve the ambiguity, we measured spectra of CpU (CH1′ at 5.85 ppm and UH1′ at 5.90 ppm) which was assigned by Lee et al. (1976). We noted that over the 40–80 °C range, δ for UH1′ was independent of temperature for CpU, consistent with our observation of UH1′ in A-G-C-U over the same temperature range where mostly single-strand forms predominate (Figure 3b). By contrast CH1′ in CpU moves substantially upfield upon decreasing temperature as does CH1′ in A-G-C-U (Figure 3a). The overall assignment is in very good agreement with the similar molecule A-A-G-C-U (Borer et al., 1975).

A-C-G-U. The complete and unambiguous assignment of the ApC resonances was made by Ezra et al. (1977) by using selective deuteration. The assignments for ApCp in the present study are in full agreement. The AH8 and AH2 protons were unambiguously assigned by their deuterium-exchange rates as given for ApG above. The CH5 of ApCp was unambiguously assigned by using homonuclear decoupling from CH6. The GH8 of A-C-G-U was unambiguously assigned by its exchange rate and comparison to ApGp and GpU data. The CH6 and UH6 of A-C-G-U were unambiguously assigned by using J_{5-6} data. Again, the CH5 and UH5 protons of A-C-G-U were unambiguously assigned by using homonuclear decoupling information. The GH1′ and UH1′ protons were assigned by using chemical shift values for GpU (E. Bubienko, unpublished results) which are in agreement with the complete and unambiguous assignment of Lee et al. (1976). Additional support for the GH1′ and UH1′ assignments is given by $J_{1'-2'}$ data where UH1′ has a consistently lower coupling constant than GH1′ in both A-C-G-U and GpU.

Acknowledgments

We are grateful to Dr. John Wright, University of California at San Diego, Dr. Jerry Dallas, University of California at Davis, and Dr. William R. Croasman, California Institute of Technology, for assistance in obtaining some of our NMR spectra. We thank Dr. M. P. Stone for assistance in obtaining some of our NMR spectra and for helpful discussions and G. D. McFarland for assistance and helpful discussions of synthetic procedures.

References

Arnott, S., Hukins, D. W. L., Dover, S. D., Fuller, W., & Hodgsen, A. R. (1973) *J. Mol. Biol. 81*, 107.

Arter, D. B., & Schmidt, P. G. (1976) *Nucleic Acids Res. 3*, 1437.

Borer, P. N. (1972) Ph.D. Thesis, University of California, Berkeley, CA.
Borer, P. N. (1975) in *Optical Properties of Nucleic Acids, Absorption and Circular Dichroism Spectra* (Fasman, G. D., Ed.) Handb. Biochem. Mol. Biol. 1, p 389, CRC Press, Cleveland, OH.
Borer, P. N., Kan L. S., & Ts'o, P. O. P. (1975) *Biochemistry 14*, 4847.
Chandrasekaran, R., Arnott, S., Banerjee, A., Campbell-Smith, S., Leslie, A. G. W., & Puigjaner, L. (1980) in *Fiber Diffraction Methods* (French, A. D., & Gardner, K. H., Eds.) ACS Symp. Ser. No. 141, p 483, American Chemical Society, Washington, D.C.
Dhingra, M. M., & Sarma, R. H. (1979) in *Stereodynamics of Molecular Systems* (Sarma, R. H., Ed.) p 15, Pergamon Press, New York.
Everett, J. R., Hughes, D. W., Bell, R. A., Alkema, D., Neilson, T., & Romaniuk, P. J. (1980) *Biopolymers 19*, 557.
Ezra, F. S., Lee, C., Kondo, N. S., Danyluk, S. S., & Sarma, R. H. (1977) *Biochemistry 16*, 1977.
Giessner-Prettre, C., & Pullman, B. (1976) *Biochem. Biophys. Res. Commun. 70*, 578.
Giessner-Prettre, C., & Pullman, B. (1977a) *J. Theor. Biol. 65*, 171.
Giessner-Prettre, C., & Pullman, B. (1977b) *J. Theor. Biol. 65*, 189.
Giessner-Prettre, C., Pullman, B., Borer, P. N., Kan, L. S., & Ts'o, P. O. P. (1976) *Biopolymers 15*, 2277.
Holbrook, S. R., Sussman, J. L., Warrant, R. W., & Kim, S. H. (1978) *J. Mol. Biol. 123*, 631.
Hughes, D. W., Bell, R. A., England, T. E., & Neilson, T. (1978) *Can. J. Chem. 56*, 2243.
Kallenbach, N. R., & Berman, H. M. (1977) *Q. Rev. Biophys. 10*, 138.
Kan, L. S., Kast, J. R., Ts'o, D. Y., & Ts'o, P. O. P. (1979) *Comput. Programs Biomed. 10*, 16.
Kearns, D. R. (1977) *Annu. Rev. Biophys. Bioeng. 6*, 477.
Lee, C., Ezra, F. S., Kondo, N. S., Sarma, R. H., & Danyluk, S. S. (1976) *Biochemistry 15*, 3627.
Martin, F. H., Uhlenbeck, O. C., & Doty, P. (1971) *J. Mol. Biol. 57*, 201.
McFarland, G. D., & Borer, P. N. (1979) *Nucleic Acids Res. 7*, 1067.
Romaniuk, P. J., Neilson, T., Hughes, D. W., & Bell, R. A. (1978) *Can. J. Chem. 56*, 2249.
Stone, M. P., Johnson, D., & Borer, P. N. (1981) *Biochemistry 20*, 3604.
Thach, R. E. (1966) *Procedures in Nucleic Acid Research* (Cantoni, G. L., & Davies, D. R., Eds.) Harper and Row, New York.
Ts'o, P. O. P. (1974) in *Bases, Nucleosides, and Nucleotides* (Ts'o, P. O. P., Ed.) Basic Princ. Nucleic Acid Chem., 1, pp 541, 547, Academic Press, New York.
Uhlenbeck, O. C., Martin, F. H., & Doty, P. (1971) *J. Mol. Biol. 57*, 217.
Van Geet, A. L. (1968) *Anal. Chem. 40*, 2227.
Van Geet, A. L. (1970) *Anal. Chem. 42*, 679.

Solution Dimensions of the Gramicidin Dimer by Dynamic Light Scattering†

S. Michielsen‡ and R. Pecora*

ABSTRACT: Gramicidin is thought to form dimeric helical rods in alcohol solutions. In addition, there is evidence that the rod dimensions change upon addition of potassium ions. The present work reports values for the translational and rotational diffusion coefficients of gramicidin in methanol and 95% ethanol and in these same solvents with added KSCN. Solution dimensions are calculated from the diffusion coefficients. The results suggest that gramicidin exists primarily as dimers in these solutions and that the gramicidin rod does indeed become shorter upon addition of potassium ion. These results are consistent with those obtained from X-ray studies on single crystals grown from alcohol solutions.

Gramicidin is a linear pentadecapeptide antibiotic from the bacterium *Bacillus brevis* with alternating L and D amino acid residues. Gramicidin facilitates the diffusion of monovalent cations across membranes by forming NH-terminal to NH-terminal helical dimers (Weinstein et al., 1979) which span the membrane and have a 5–7 Å diameter channel down the center of the helix, through which the monovalent cations can flow. Anions do not flow through these channels whereas divalent cations block the channel and hence prevent further diffusion of monovalent cations through the membranes (Weinstein et al., 1979; Haydon & Hladky, 1972; Veatch & Stryer, 1977; Urry, 1971; Bamberg et al., 1978). X-ray diffraction studies on gramicidin A grown from methanol and ethanol solutions show helical rods with repeat units of 32 Å with 14–16-Å diameters and channels of 4.5–5-Å diameter. Similar studies on gramicidin A complexed to cesium or potassium ions show the helical rods to have repeat units of only 26 Å with 16-Å diameters and 6.8 Å diameter channels (Koeppe et al., 1978, 1979). Fossel et al. (1974) used ^{13}C NMR spectroscopy to determine the rotational relaxation time for gramicidin in methanol, for which they obtained $\tau_R = 25$ ns. This is much too slow for a dimer of the dimensions given above.

The present study utilizing dynamic light scattering (DLS) was undertaken to determine whether or not gramicidin exists primarily in dimeric form in solution and, if so, to determine

† From the Department of Chemistry, Stanford University, Stanford, California 94305. *Received April 28, 1981.* This work was supported in part by grants from the National Institutes of Health (2 R01 GM22517) and the National Science Foundation (CHE 79-01070).
‡ Present address: Experimental Station, E. I. du Pont de Nemours and Co., Inc., Wilmington, DE 19898.

0006-2960/81/0420-6994$01.25/0